19F MRI QUANTIFICATION USING B1 CORRECTION

Ina Vernikouskaya[1], Alexander Pochert[2], and Volker Rasche[1]
[1]*Internal Medicine II, University Hospital of Ulm, Ulm, Baden-Wuerttemberg, Germany,* [2]*Inorganic Chemistry II, University of Ulm, Ulm, Baden-Wuerttemberg, Germany*

TARGET AUDIENCE: Researchers interested in the quantification of ^{19}F MRI signal at high field with inhomogeneous excitation field.

PURPOSE: The signal intensity in ^{19}F MRI images can be quantified by comparing the signal intensity to that of a reference sample. One issue, however, can arise from the sensitivity profile of the used coil. If at low field strengths producing a uniform excitation field is theoretically possible, the difficulties are especially encountered at high field strengths, where an inhomogeneous profile of the excitation field B_1^+ can lead to wrong quantitative results. Many of existing B_1^+ mapping methods suffers from: T_1 dependence[1], long acquisition times[2], cancelling of the signal during saturation[3,4], inaccuracy at low flip angles[2,5], and require modified imaging sequences[5,6]. In this work we apply the fast and accurate method to map the B_1^+ field, similar to those introduced by Sung et.al[7], for correction of ^{19}F MRI signal of perfluoro-15-crown-5-ether (PFCE) at 11.7T Bruker BioSpec small animal MRI system.

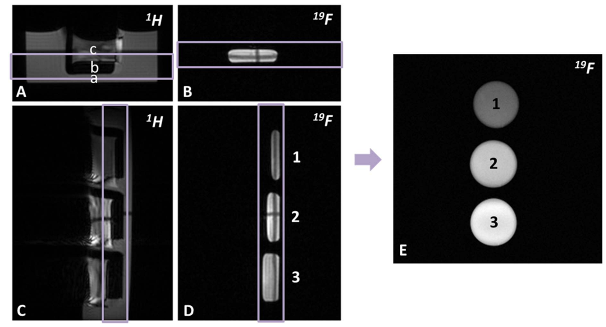

Figure 1. ^{1}H (A, C) and ^{19}F (B, D) MR images of the agarose phantom containing three openings (1-3) filled with agarose gel (a), PFCE (b), and cycloxehane (c) acquired in axial (A, B) and sagittal (C, D) orientation. The dislocation of the cyclohexane slice (c) in ^{1}H image is due to the chemical shift artifact. (E) ^{19}F image of 5-mm thick slice acquired in geometry indicated in purple rectangles in images (A-D).

METHODS: The method is based on the **S**poiled **G**radient **E**cho **S**equence (*SPGR*), where the signal intensity $I_{\alpha n}$ for a nominal flip angle α_n can be expressed as: $I_{\alpha_n} = M_0 \frac{\sin(B_1\alpha_n)(1-E)}{1-E\cos(B_1\alpha_n)}$, where M_0 is the longitudinal magnetization at thermal equilibrium, B_1 is a relative flip angle variation, defined by ratio between the actual flip angle and the prescribed flip angle, and $E = e^{-TR/T_1}$. Then taken the ratio of two signal magnitudes at two different flip angles, B_1 can be numerically calculated. Transverse relaxation is not included in the equation because the T_2/T_2^* effect will only scale the signal amplitude and does not affect the signals ratio. The proposed method relies on the assumption that T_1 is well-known and constant across the region of interest. To calculate the T_1 value of PFCE ^{19}F inversion recovery curve was fitted with the 3-parameters model. The SPGR sequence optimization was done on a pure PFCE phantom, the results were compared with the simulation prediction for defined T_1 time. Since PFCE is not soluble in standard solvents, a phantom with different volumes of PFCE instead of different concentrations was used for B_1 mapping and for quantification of ^{19}F signal (Fig. 1: 1 - 200µL, 2 - 300µL, 3 - 400µL). For B_1^+ mapping two images at 25° and 15° were acquired with the optimized SPGR sequence. Intensity of the acquired image was corrected in three ways: 1) accounting for transmit field (denoted as B_1^+) only; 2) accounting for receive field (B_1^-) only, and 3) accounting for transmit/receive fields (B_1^+/B_1^-). 5-mm thick slice was acquired for ^{19}F signal quantification; so that the variations of ^{19}F signal intensity in Fig. 1 E is proportional to the PFCE volume.

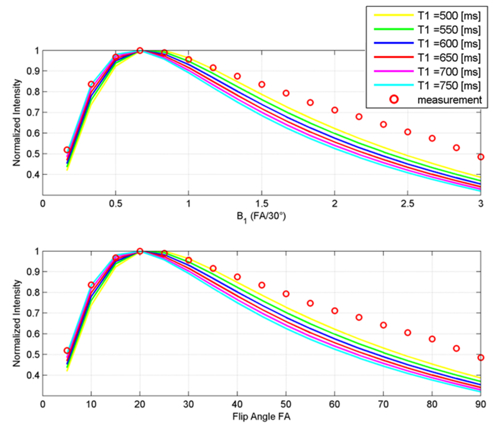

Figure 2: Simulation of the SPGR-signal acquired at TR = 40ms for different T_1 relaxation times with B_1 values in the range of 0.15 to 3.0 corresponding to FAs from 5° to 90° vs. MR measurement with SPGR sequence at different nominal FAs.

RESULTS: Fitting of the inversion recovery data from the PFCE phantom yielded a T_1 value of 650ms. Very good correlation between the measurement with the optimized SPGR sequence (FOV 4x4cm, 2mm slice, 256^2 matrix, TR/TE = 40/3.9ms, BW 50kHz, 4 NEX, long read/slice spoiler, 0:41min scan time) and simulation prediction for T_1 = 650ms can be observed for flip angles (FA) up to 30° (Fig. 2). The differences between simulation and measurement at higher FAs is due to impact of T_2/T_2^* effects which are not taken into account in the simulation of SPGR sequence. Fig. 3 summarizes results in quantification phantom in form of intensity images and intensity profiles through the middle of correspondent intensity image along the vertical line. The B_1 profile (Fig. 3b) shows its typical behavior with its maximum intensity in the coil center and intensity decrease aside the coil center. B_1^+/B_1^- correction appeared to perform best in the image intensity correction (Fig. 3c), demonstrating decrease in the signal intensity in the coil center and increase of it aside the coil center. Relative quantification on the base of 25° intensity image relating three ROIs indicated in Fig. 3a to each other (theoretically: ROI2/ROI1 = 1.5, ROI3/ROI1 = 2.0, ROI3/ROI2 = 1.33), gives following values: 1.98, 2.28, 1.15 for non-corrected image; 2.19, 2.38, 1.09 for B_1^+ only corrected image; 1.45, 1.9, 1.31 for B_1^- only corrected image; and 1.6, 1.99, 1.24 for B_1^+/B_1^- corrected image.

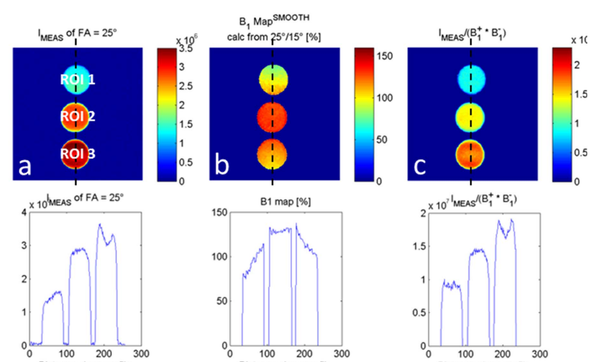

Figure 3: MR intensity image acquired at flip angle of 25° (a) is corrected in (c) with B_1 map in (b) calculated with assumed T_1 of 650 ms from the signal ratio of 25°/15°. Intensity profiles below respective intensity images are along the indicated dotted line.

DISCUSSION & CONCLUSION: The proposed B_1 mapping method is promising solution for ^{19}F application, because (1) T_1 of *e.g.* PFCE can be well-characterized and is constant; (2) only voxels containing ^{19}F signal should be corrected (global map is not necessary); (3) method is not time-consuming. Estimation error for the relative quantification after B_1^+/B_1^- - correction is within 6-7%.

REFERENCES: (1) F. Jiru und U. Klose, MRM 2006. (2) E. K. Insko und L. Bolinger, JMR 1993. (3) C. H. Cunningham et al., MRM 2006. (4) N. G. Dowell und P. S. Tofts, MRM 2007. (5) V. L. Yarnykh, MRM 2007. (6) L. I. Sacolick et al., MRM 2010. (7) K. Sung et al., MRM 2013.